JOURNAL OF MATERIALS SCIENCE **38** (2003) 1391 – 1396

Phase formation kinetics of nanoparticle-seeded strontium bismuth tantalate powder

G. M. ANILKUMAR
Advanced Materials Research Center (AMRC), Daejin University, Pochun-koon, Kyunggi-do, 487-711, Korea (South)

YUN-MO SUNG*
Functional Nanostructured Materials Laboratory (FNML), Department of Materials Science & Engineering, Daejin University, Pochun-koon, Kyunggi-do, 487-711, Korea (South)
E-mail: ymsung@road.daejin.ac.kr

Strontium bismuth tantalate (SBT) having composition of $Sr_{0.7}Bi_{2.3}Ta_2O_9$ has been prepared through sol-gel method using their corresponding metal alkoxides as precursors. Seeded SBT powder was prepared by the addition of 5 wt% of nanometer-sized SBT particles to the sol followed by pyrolysis. Differential thermal analyses (DTA) were performed on the unseeded and seeded powder and Aurivillius phase formation temperatures were found to be reduced by ~60°C in the seeded ones. Non-isothermal kinetic analyses were applied to the DTA results to obtain activation energy and Avrami exponent values for the Aurivillius phase formation in unseeded and seeded samples. The activation energy for the Aurivillius phase formation was found to be ~268 kJ/mol for the seeded ones, while ~375 kJ/mol for the unseeded ones, which plays a major role for the enhanced kinetics in the seeded ones. The Avrami exponent values for the Aurivillius phase formation in unseeded and seeded ones were determined as ~2.80 and ~1.15, respectively, revealing different nucleation and crystal growth mechanisms.

1. Introduction

Ferroelectrics are excellent candidates for applications in data storage in digital memory systems, in addition to its many other important applications such as piezoelectrics, pyroelectrics, and electro–optics for sensors and actuators [1, 2]. Among the various ferroelectric materials, the bismuth based, layer structured perovskite compounds, belonging to the so-called Aurivillius class of layered perovskites, have attracted much attention in recent years [3]. In comparison to various isotropic perovskite ferroelectrics, strontium bismuth tantalate (SBT) has been identified for potential applications, especially in the field of non-volatile ferroelectric random access memories (NvFRAM) [4]. This is basically because of its properties such as excellent retention characteristics, low leakage current and almost polarization fatigue free operation for up to $\sim 10^{12}$ switching cycles [4]. Out of the various methods reported for the preparation of such materials, sol-gel method is found to be a promising one. Since the starting materials are mixed in a molecular level in the solution, a high degree of homogeneity is obtained, resulting in low temperature crystallization [5, 6]. Another advantage is that trace elements can be successively introduced into the sol, which allows the tailoring of the process to specific requirement [5]. Several attempts have been made to synthesize SBT at a low temperature and to improve the microstructure and hence ferroelectric properties [7, 8]. Even though the possible existence of many non-stoichiometric phases, which are stable within the (Sr-Bi-Ta-O) system, has been reported, SBT systems with a near stoichiometric composition ($Sr_{1-x}Bi_{2+y}Ta_2O_9$) have been found to show significantly improved ferroelectric properties [9]. It has been reported that Bi substitution and cation vacancy formation at the strontium sites enhance the structural distortion of the TaO_6 octahedra, leading to a larger ferroelectric spontaneous polarization [10]. However, layered perovskite ferroelectrics suffer from two limitations: a relatively low remnant polarization and a relatively high processing temperature. In order to reduce the transformation temperature and to refine the microstructure the effect of perovskite seeds has been studied in the fields of sol-gel derived $PbTiO_3$ and $Pb(Zr, Ti)O_3$ (PZT) systems [11, 13], since an addition of perovskite seed particles causes an increase in the number of nucleation sites for phase transformation. The effective method of controlling the particle size, as well as reaction kinetics is by introducing crystallographically preferred nucleation sites in the form of seed particles into a system [14]. The transformation temperature can also be reduced by the seeding process. For example, Messing *et al.* [15] observed a reduction in the transformation temperature of α-alumina

*Author to whom all correspondence should be addressed.

seeded boehmite system. Further, a reduction in the perovskite formation temperature has been reported with the addition of $BaTiO_3$ seed particles in the lead magnesium niobate (PMN) system, because of epitaxial effects [16]. Recently, a non-isothermal kinetic analysis was carried out by Sung [17] to determine the activation energy and Avrami exponent for the phase formation reactions in the SBT system. However, the effect of nucleating seeds in the above system has not been reported.

The present paper describes the synthesis of seeded $Sr_{0.7}Bi_{2.3}Ta_2O_9$ (SBT) precursor and their phase formation characteristics. The crystallization characteristics were analyzed using differential thermal analysis (DTA). Nonisothermal kinetic analyses were applied to the DTA results to determine the activation energy and Avrami exponent. Finally, a comparison has been made with crystallization behavior of the unseeded SBT.

2. Experimental

SBT sol was prepared using the precursors such as Sr-isopropoxide (Aldrich Chemicals, Milwaukee, WI), Bi-t-amyloxide and Ta-ethoxide (High Purity Chemicals Co., Osaka, Japan). All these alkoxides were handled in a glove box under dried Ar atmosphere. 2-Methoxyethanol, the most extensively used solvent in the perovskite preparation [18], was used as the solvent in the SBT sol preparation. Sr-isopropoxide was dissolved in 2-methoxyethanol by refluxing it at 130°C followed by distillation. Bi-t-amyloxide was added to the above solution followed by refluxing it at 60°C and distillation at 110°C, so that Sr-Bi double alkoxide solution was formed. Ta-ethoxide is dissolved in 2-methoxyethanol by refluxing at 130°C. This solution was further refluxed with Sr-Bi double alkoxide solution and concentrated to get 0.1 M SBT stock solution.

SBT seed particles were prepared by heating the SBT gel at a temperature of 800°C for 2 h and the perovskite phase formation was confirmed using X-ray diffraction (XRD). The powder obtained was further ball milled in 2-methoxyethanol medium for 5 h. In order to get a good dispersion of the seed particles, the pH of the suspension was adjusted to ∼4 by the addition of acetic acid (Aldrich Chemicals, Milwaukee, WI). The suspension obtained was further ultrasonicated and the fines from this lot were separated by sedimentation. The seed suspension prepared had a concentration of 2.1 mg/ml. Seeded SBT precursor gel was prepared by adding nucleating seeds of SBT (5 wt%) suspension (seed size of ∼60–80 nm) to the precursor sol and the viscosity was raised by adjusting the pH of the sol to ∼7.5 using ethylene diamene (Aldrich Chemicals, Milwaukee, WI), so that the seed particles are homogeneously dispersed in the gel matrix. In order to find out the pyrolysis temperature, thermo gravimetric analysis (TGA) was carried out at a heating rate of 10°C/min, on the SBT gel dried at 150°C for 1 h. The seeded and unseeded gel obtained by drying at 150°C was further preheated at 500°C for 1 h in order to obtain non-crystalline SBT powder. The particle size distribution of the final non-crystalline SBT powder including nanometer-sized seed particles was 10–30 μm. The whole process for the preparation of seeded/unseeded SBT precursor is presented in Fig. 1.

Differential thermal analysis of the seeded and unseeded powders were carried out using DTA (SETARAM-TGDTA 92, Lyon, France) at scan rates of 10, 15, 20 and 30°C/min, up to 910°C and after reaching the desired temperature it is cooled down to room temperature at a rate of ∼90°C/min. Non-isothermal kinetic analysis was applied to the DTA results to determine the crystallization behavior of the seeded and unseeded SBT precursor.

3. Results and discussion

Thermogravimetric analysis (TGA) curve of the SBT precursor is presented in Fig. 2. The curve shows two-step weight loss. The first weight loss in the temperature range of 150–250°C, corresponds to the removal of the remaining solvent from the gel network, while the second weight loss in the range of 250–500°C is due to the removal of the organic materials during heat treatment. From the TGA data the pyrolysis temperature is fixed as 500°C, to obtain the non-crystalline SBT gel powder. Therefore, the DTA analyses of the precursors were carried out after pyrolyzing the gel at 500°C for 1 h.

DTA curves of unseeded and seeded SBT precursors with different heating rates (10, 15, 20 and 30°C/min) are presented in Fig. 3. The Aurivillius phase formation temperatures of unseeded and seeded SBT precursors with respect to different scan rates are presented in Table I. Two exotherms were identified in the DTA curves. Earlier studies indicate that the Aurivillius phase in SBT system is formed through an intermediate phase known as fluorite [17]. Therefore, the first exotherm appearing in the DTA curves corresponds to the formation of the intermediate fluorite phase, while the second exotherm indicates the transformation from fluorite to Aurivillius phase. For unseeded samples, the formation of fluorite phase is indicated by a broad exotherms ranging from 635 to 675°C in the DTA curve, while the first exothems indicating the formation of fluorite phase are relatively small in the seeded samples. Comparing the Aurivillius phase formation temperatures for the seeded and unseeded precursors, the formation of Aurivillius phase is indicated by a sharp exotherm at 710–742°C in the seeded sample while at 771–799°C for the unseeded one under the same DTA scan conditions. Thus, ∼60°C reduction in formation temperature is observed for the seeded samples, which implying the enhanced phase formation kinetics in the seeded ones.

TABLE I The Aurivillius phase formation temperatures (T_p) of the unseeded and seeded SBT precursor with respect to different scan rates

	T_p (°C)	
Scan rate (°C/min)	Unseeded	Seeded
10	771	710
15	779	722
20	786	731
30	799	742

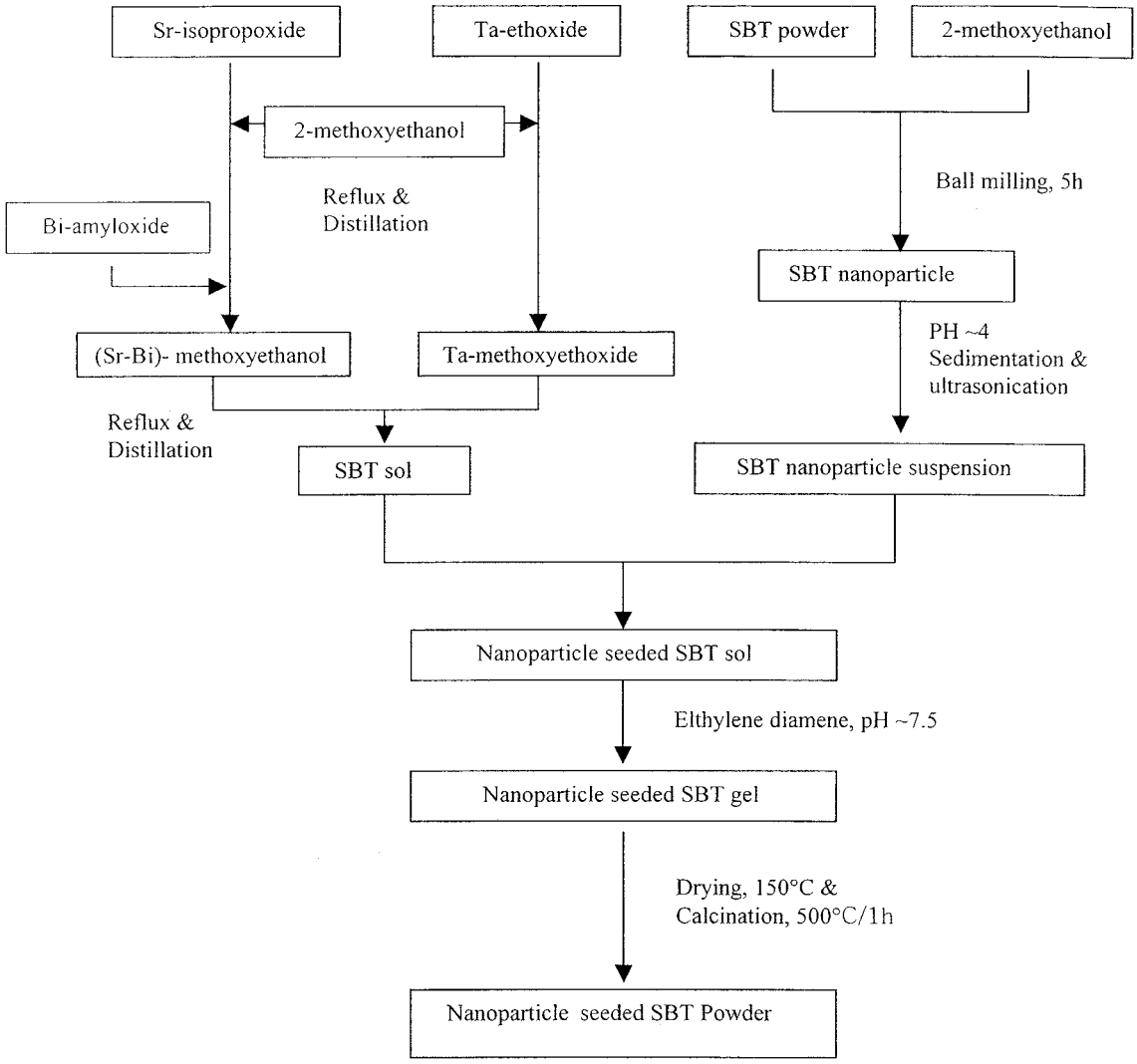

Figure 1 A flow chart for the preparation of seeded SBT powder.

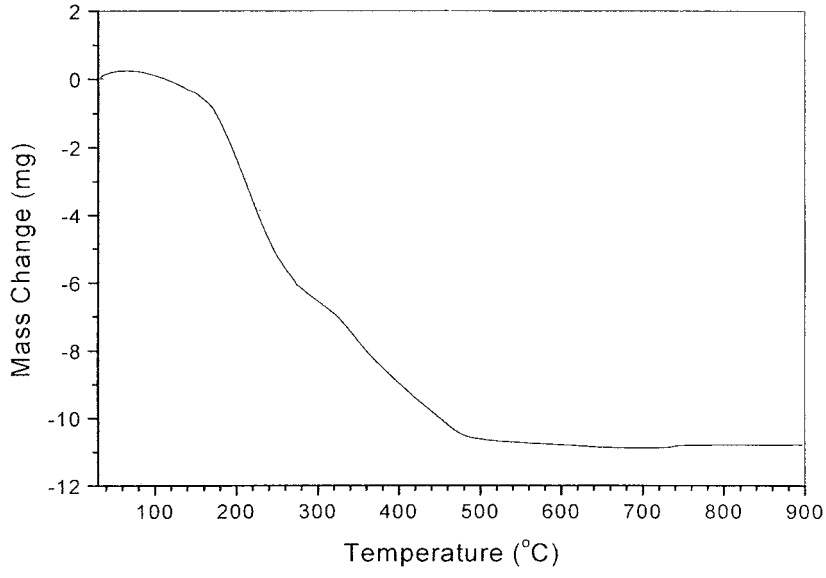

Figure 2 A thermogravimetric analysis (TGA) curve of SBT gel.

The DTA results were further subjected to kinetic analyses in order to find out the activation energy and the Avrami exponent values. Although most of the kinetic studies are carried out isothermally due to ease of data analysis in terms of the Johnson-Mehl-Avrami (JMA) equation [19], isothermal treatments have some disadvantages. If the selected temperature is too high, the crystallization may start before reaching the isothermal condition, and if it is too low, the crystallization may be too sluggish and can not be accurately

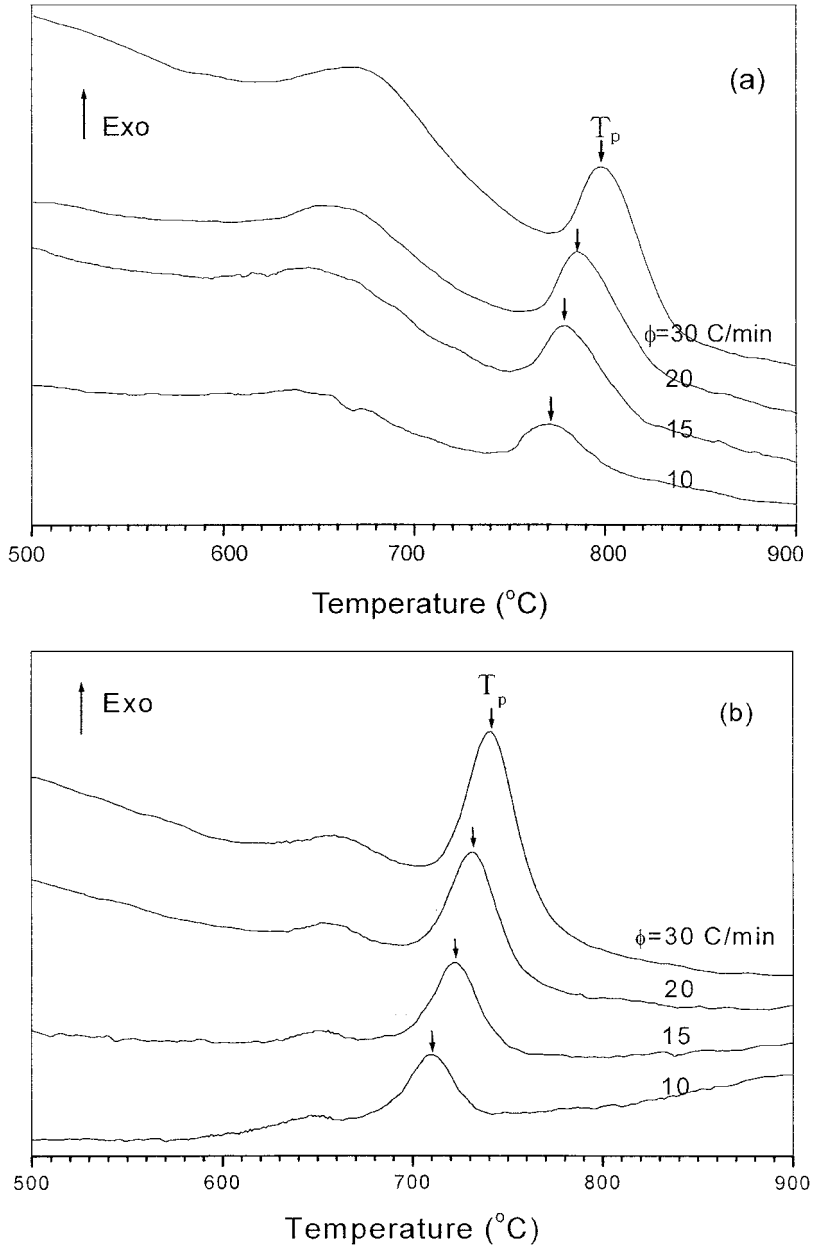

Figure 3 Differential thermal analysis (DTA) curves of (a) unseeded and (b) seeded SBT precursors.

determined. Several non-isothermal techniques have been proposed which are quicker and less sensitive to previous and next transformations. In addition, they can provide more accurately the activation energy and crystal growth mode. Non-isothermal data are typically interpreted using Kissinger equation [20],

$$\ln\left(\frac{\phi}{T_p^2}\right) = -\frac{Q}{RT_p} + \text{const.} \tag{1}$$

Here, ϕ is the DTA scan rate, Q is the activation energy for the phase transformation, T_p is the transformation peak temperature and R is the gas constant. Fig. 4 shows the Kissinger plots of unseeded and seeded SBT powder. From the slope of the curves, the activation energy values of the Aurivillius phase were determined as ∼375 and ∼268 kJ/mol for the unseeded and seeded ones, respectively.

The Avrami exponent, n, can be evaluated by Ozawa equation [21]. First, the volume fraction of phase transformation x, at the same temperature, T, from four crystallization exotherms under different heating rates is calculated by the ratio of partial area at T to the total area of crystallization exotherm. After plotting $\ln[-\ln(1-x)]_T$ vs. $\ln\phi$ and if the data can be fitted to the linear function, then the slope of the function is $-n$, i.e.

$$\frac{d\ln[-\ln(1-x)]}{d\ln\phi} = -n \tag{2}$$

Fig. 5 represents the Ozawa plots of unseeded and seeded powder. From the slope of the curves, the Avrami exponent (n) values were determined. For the seeded one, the n values corresponding to Aurivillius formation are found to be ∼2.8, while for its counterpart it is ∼1.15. The Avrami exponent value of ∼1 implies surface nucleation and crystal growth mechanism, while that of ∼3 implies bulk nucleation and crystal growth mechanism. The Avrami exponent value of ∼3 in the seeded samples implies that the nucleation of Aurivillius phase occurs at the nanoseeds/fluorite

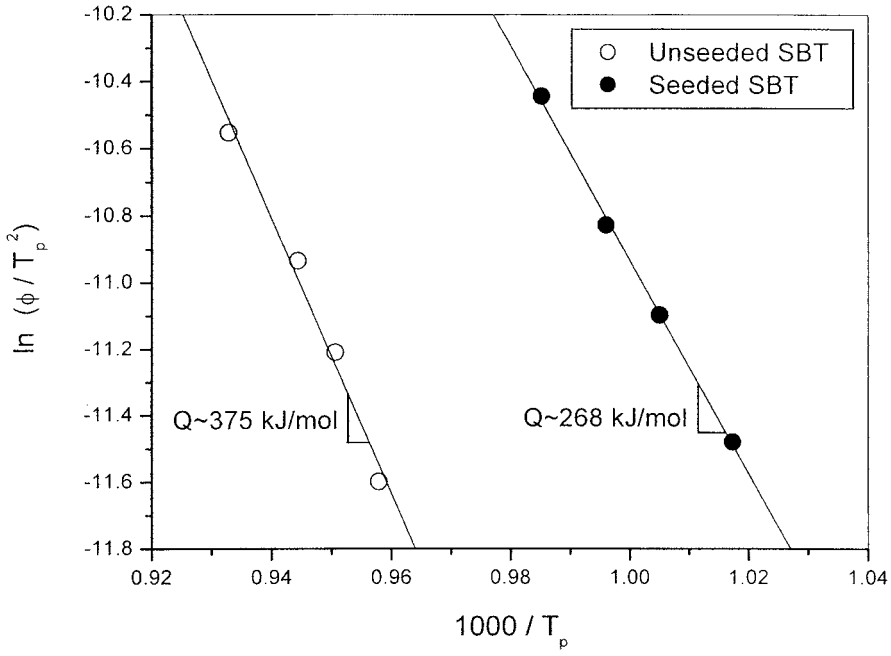

Figure 4 Kissinger plots indicating the activation energy involved in the fluorite-to-Aurivillius transformation of unseeded and seeded SBT powder.

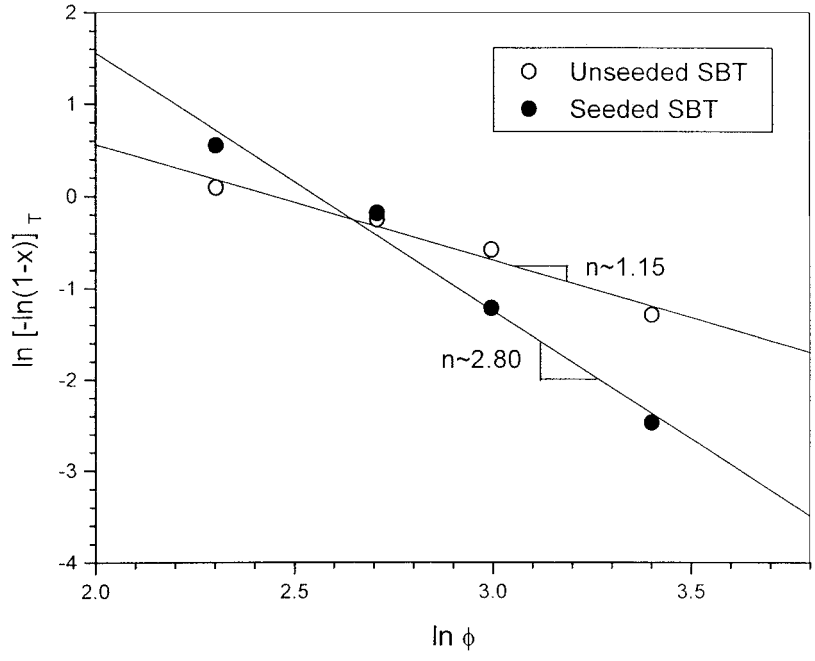

Figure 5 Ozawa plots indicating the Avrami exponent involved in the fluorite-to-Aurivillius transformation of unseeded and seeded SBT powder.

interfaces. The nanoseeds, finely distributed inside of each particle, induce the epitaxial nucleation and growth of Aurivillius phase and thus bulk nucleation and crystal growth. On the other hand, the unseeded samples do not have preferential sites for the Aurivillius nucleation except the particle surface which is in high energy level compared to the inner bulk portion. Thus, surface nucleation and subsequent crystal growth from the surface of each particle is expected in the case of unseeded samples. The effect of nanoparticles on the nucleation and crystallization mode of Aurivillius phase is highly distinct in seeded samples. Table II shows the activation energy and Avrami exponent values for Aurivillius phase formation.

The nucleation and growth process is known to be associated with transformation from amorphous gel to the final perovskite phase and introduction of nanometer-sized ceramic particles of isostructural nature enhances the crystallization of the final phase. Earlier studies on reaction kinetics also have shown that the phase transformation, pyrochlore/fluorite-to-perovskite, is a nucleation-controlled process and the nucleation of the perovskite phase is the rate-controlling step of the

TABLE II A comparison between the activation energy (Q) and Avrami exponent (n) for the seeded and unseeded SBT precursor for the Aurivillius phase formation

Powder	Activation energy (kJ/mol)	Avrami exponent
Unseeded	375	1.15
Seeded	268	2.80

reaction [11–13]. Therefore, it is possible to increase the reaction kinetics if the number of nucleation sites is increased.

Seeding in sol-gel systems refers to the introduction of nanoparticles of the thermodynamically stable phase or its isostructural counterparts as a method for enhanced transformation kinetics, densification and microstructural refinement [15]. The weight fraction of seed particles that are required to obtain a high seed concentration in the precursor is inversely related to the particle size, hence it is important to use nanometer-sized particles as seeds. Therefore, in the present work the seeding effects can be explained by the fact that the introduction of nanometer-sized SBT perovskite seed particles (average particle size of ∼60–80 nm) introduces nucleation sites in the form of low-energy epitaxial interfaces and thereby selectively increases the crystallization rate of the phase which is isostructural with the seed particles. This was supported by the kinetic analysis that the activation energy involved in the fluorite-to-Aurivillius transformation is ∼268 kJ/mol for the seeded and ∼375 kJ/mol for the unseeded, showing a reduction of ∼107 kJ/mol for the seeded SBT sample. The phase transformation sequence is also found to be different, for example, as mentioned earlier, the first exotherm appearing at ∼675°C indicating the formation of fluorite is very clear in the DTA pattern of the unseeded SBT gel. However, such a distinct exotherms are not seen in the seeded one. This may be explained by the fact that since during heat treatment, when fluorite nuclei starts forming and growing from the amorphous gel, the SBT perovskite seeds already present, the fluorite crystals eventually transform to the final Aurivillius phase. This indicates the high instability of the fluorite phase and a more homogenous reaction to form the Aurivillius phase. This was further supported by the low activation energy value for the fluorite-to-Aurivillius phase formation in the seeded precursor. It has been reported that in the case of heterogeneous nucleation process, the presence of nanometer-sized seed particles requires a much smaller activation energy to reach the critical nuclei size [22]. In addition to this, Moon *et al.* [23] reported that the intermediate phases such as pyrochlore or fluorite phases in oriented lead titanate can be avoided by particle seeding and was further supported by the work of Tartaj *et al.* [12]. In the present case, also the introduction of nanometer-sized SBT seed particles influenced the crystallization process by lowering the crystallization temperature, mainly by enhancing the crystallization kinetics at each temperature. Therefore, it can be stated that the increased rate of Aurivillius formation and lowered activation energy in the seeded SBT gel depressed the presence of the intermediate fluorite phase, resulting in the formation of the perovskite phase at a lower temperature.

4. Conclusions

Seeded SBT precursor was prepared by introducing 5 wt% of nanometer-sized SBT particles into the SBT precursor sol. The phase formation characteristics of the seeded precursor were compared with the unseeded one. Enhanced crystallization kinetics was observed for the seeded sample resulting in the formation of the Aurivillius phase at a lower temperature. Activation energy measurements showed a reduction of ∼100 kJ/mol for the seeded compared with the unseeded sample. Seeding was found to be effective only for the Aurivillius phase formation by supplying nucleation sites in the form of low-energy epitaxial interfaces. The low activation energy and enhanced reaction kinetics of the seeded system also depressed the presence of the fluorite intermediate phase in the seeded system. Thus by controlling the nucleation kinetics in the sol-gel system using the appropriate seed nuclei it may be possible to reduce or even avoid the thermodynamically metastable phases, thereby lowering the formation temperature of the final perovskite phase.

Acknowledgments

This work was supported by grant No. (R05-2001-000-00810-0) from Basic Research Program of the Korea Science and Engineering Foundation (KOSEF). One of the authors (Gopinathan M. Anilkumar) acknowledges KOSEF for the financial support through "Post Doctoral Fellowships for Foreign Researchers" program in 2001.

References

1. G. H. HAERTLING, *J. Amer. Ceram. Soc.* **82** (1999) 797.
2. A. I. KINGON and S. K. STREIFFER, *Current Opinion in Solid State and Mater. Che.* **4** (1999) 39.
3. T. ATSUKI, N. SOYAMA, T. YONEZEWA and K. OGI, *Jpn. J. Appl. Phys.* **34** (1995) 5096.
4. J. F. SCOTT, F. M. ROSS, C. A. PAZ DE ARAUJO, M. C. SCOTT and M. HUFFMAN, *Mater. Res. Soc. Bull.* **21** (1996).
5. A. C. PIERRE, "Introduction to Sol-Gel Processing" (Kluwer Academic Publishers, Boston, MA, 1998) p. 5.
6. G. YI and M. SAYER, *Amer. Ceram. Soc. Bull.* **70** (1991) 1173.
7. R. JAIN, V. GUPTA and K. SREENIVAS, *Mater. Sci. & Eng.* B **78** (2000) 63.
8. K. KATO, C. ZHENG, J. M. FINDER, S. K. DEY and Y. TORII, *J. Amer. Ceram. Soc.* **81** (1998) 1869.
9. Y. TORII, K. TATO, A. T. SUZUKI, H. J. HWANG and S. K. DEY, *J. Mater. Sci. Lett.* **17** (1998) 827.
10. Y. SHIMAKAWA, Y. KUBO, Y. NAKAGAWA, T. KAMIYAMA, H. ASANO and F. IZUMI, *Appl. Phys. Lett.* **74** (1999) 1904.
11. A. WU, I. M. M. SALVADO, P. M. VILARINHO and J. L. BAPTISTA, *J. Eur. Ceram. Soc.* **17** (1997) 1443.
12. J. TARTAJ, C. MOURE and P. DURAN, *Ceram. Int.* **27** (2001) 741.
13. A. TOWATA, H. J. HWANG, M. YASNOKA and M. SANDO, *J. Mater. Sci.* **35** (2000) 4009.
14. N. S. BELL, S. B. CHO and J. H. ADAIR, *J. Amer. Ceram. Soc.* **81** (1998) 1411.
15. M. KUMAGAI and G. L. MESSING, *ibid.* **68** (1985) 500.
16. Y. NARENDAR and G. L. MESSING, *ibid.* **82** (1999) 1659.
17. Y.-M. SUNG, *J. Mater. Res.* **16** (2001) 2039.
18. C. H. LUCK, C. L. MAK and K. H. WONG, *Thin Solid Films* **298** (1997) 57.
19. M. AVRAMI, *J. Chem. Phys.* **9** (1941) 177.
20. H. E. KISSINGER, *J. Res. Natl. Bur. Stand. (US)* **57** (1956) 217.
21. T. OZAWA, *Polymer* **12** (1971) 150.
22. J. C. HULLING and G. L. MESSING, *Ceram. Trans.* **22** (1991) 401.
23. J. MOON, J. A. KERCHNER, J. LEBLEU, A. A. MORRONE, J. H. ADAIR, *J. Amer. Ceram. Soc.* **80** (1997) 2613.

Received 29 July
and accepted 23 December 2002